Progress In Electromagnetics Research C, Vol. 60, 105–114, 2015

Outage Probability and Bit-error Rate for Communication Systems with Gaussian-Schell Electromagnetism Beams in Non-Kolmogorov Raining Turbulence

Ye Li[1], Yixin Zhang[1, 2, *], Zhengda Hu[1, 2], and Qiu Wang[1]

Abstract—Two major performance degrading factors in free space optical communication systems are rainfall and atmospheric turbulence. We study the outage probability and bit-error rate for free-space communication links with spatial diversity and Gaussian-Schell electromagnetism beams over the raining turbulence fading channels by double inverse Gaussian distribution proposed in this paper. Assuming intensity-modulation/direct detection with on-off keying and perfect channel state information, we derive expressions of average bit-error rate and outage probability of multiple-input multiple-output free space optical communication systems over double inverse Gaussian model. The effects of scintillation index of raining turbulence, spatially coherence of source, pointing errors and spectral index of non-Kolmogorov turbulence on the outage probability and bit-error rate of multiple-input multiple-output free space optical communication systems are examined.

1. INTRODUCTION

Free space optical (FSO) communication has been studied widely for its superior characteristics such as no licensing requirements, reduced interference, high security, cost-effectiveness, and simplicity of system design and deployment, and high connection. However, the factors of the atmospheric turbulence [1–7], tiny building jitter [3, 7], and rainfall [8–15] limit widespread application of FSO.

Recent progress on research of the atmospheric-induced fading has proposed many distribution models to describe the effects of atmosphere turbulence and rainfall on optical transmission. Physical-mathematical models for the prediction of rain fading distribution have been proposed in such as lognormal distribution [9], gamma distribution [10], Weibull distribution [11, 12] and inverse Gaussian (IG) [13–15]. For atmospheric turbulence fading distribution, in weak scintillation region, log-normal distribution is the most commonly used model in application [1–3, 7]. In order to mitigate the effects of atmospheric turbulence on FSO system, there have been various attempts using the multiple-input multiple-output (MIMO) technique [1, 16, 17]. Many methods have been proposed to overcome the turbulence-induced degradation of laser beams [2, 18–20]. However, there are critical defects of the log-normal distribution. The distribution of the sum of log-normal variables in MIMO FSO systems is not analytically available so as to require additional approximation in the performance analysis of channels [17, 21]. For this reason, there are no closed-form analytical expressions for bit-error rate (BER) and the outage probability of MIMO FSO systems in log-normal models, and the MIMO FSO cannot be settled real time when the turbulence-induced fading is characterized by log-normal distribution model. Recent studies have shown that the IG distribution can substitute the log-normal distribution and can be applied to MIMO FSO system [17, 21, 22]. On the other hand, rainfall is inevitable natural

Received 23 October 2015, Accepted 16 November 2015, Scheduled 9 December 2015

* Corresponding author: Yixin Zhang (zyx@jiangnan.edu.cn).

[1] School of Science, Jiangnan University, Wuxi 214122, China. [2] Jiangsu Provincial Research Center of Light Industrial Optoelectronic Engineering and Technology, China.

phenomenon, and rain attenuation prediction modeling is of utmost importance for the reliable design and performance evaluation of line-of-sight (LOS) millimeter-wave terrestrial link [13–15]. However, to the best of our knowledge, there is almost no discussion with respect to the effects of turbulence and rainfall on the probability distribution of Gaussian-Schell electromagnetism beams in raining turbulence (the coexisting of the turbulence and rainfall) fading channels.

In this paper, we apply IG statistical model of intensity fluctuations caused by turbulence and rainfall fluctuations to analyze the performance of the MIMO FSO system and propose a new distribution model of rainfall and turbulence induced fading. The outage probability and BER of the MIMO FSO channel in raining turbulence were derived based on the source of Gaussian-Schell electromagnetism beams and the intensity-modulation/direct-detection (IM/DD) with on-off keying (OOK). The paper is organized as follows. The double inverse Gaussian model of BER and outage probability in raining turbulence is proposed in Section 2. Section 3 describes the results of numerical simulations. Section 4 concludes the paper.

2. THE BER AND OUTAGE PROBABILITY

For MIMO FSO communication links (see Figure 1), the signal is transmitted by M apertures and received by N apertures over a discrete time ergodic channel with additive Gaussian noise. The communication link is a horizontal path near ground with raining turbulence and misalignment. The channel is assumed to be memoryless and stationary. The receiver integrates the photocurrent signal related to the incident optical power by the detector responsively for each bit period. Assuming a binary input and continuous output and IM/DD with OOK modulation, the received signal at the nth receiver aperture can be expressed by [1]

$$y_n = x\tau \sum_{\varpi=1}^{M} \eta_{\varpi n} + h, \quad n = 1, \ldots, N \tag{1}$$

where y_n is the received signal intensity of the nth receiver, x the modulated transmitted signal intensity (and takes values 0 or 1), τ the detection efficiency and h the signal-independent additive white Gaussian noise with zero mean and variance σ_h^2. The channel state $\eta_{\varpi n}$ models the random attenuation of the propagation channel. In our model, $\eta_{\varpi n} = \bar{\eta}_\beta \eta_\beta \eta_\alpha \eta_p$ results from the path loss caused by the absorption and scattering of rain $\bar{\eta}_\beta$, scintillation of rainfall fluctuations η_β, t fading of turbulence scintillations η_α and beam wander and the pointing errors of channel link η_p.

2.1. Model of Rain Fading Distribution

There are mainly two aspects in the influence of rainfall on the transmission beams. One is the average attenuation of light caused by the absorption and scattering of rain, and the other is the intensity fluctuations (scintillations) caused by rainfall fluctuations. The average attenuation can be described

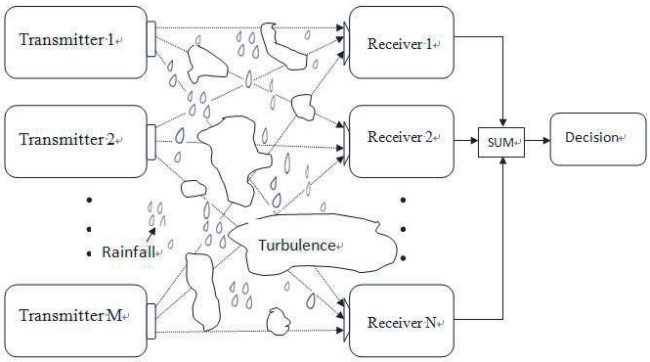

Figure 1. Block diagram of $M \times N$ FSO system over raining and atmospheric turbulence channel.

by the Beers-Lambert Law [23]

$$\bar{\eta}_\beta = \exp\left(-2.9z/V\right) \tag{2}$$

where V is the visibility and z the distance between transmitters and receivers.

The attenuation fluctuations (or fading) η_β can be modeled as inverse Gaussian distribution [13–15] in MIMO channels

$$p\left(\eta_\beta\right) = \sqrt{\frac{J^2}{2\pi\vartheta_I^2\eta_\beta^3}}\exp\left(-\frac{\left(\eta_\alpha - J\right)^2}{2\vartheta_I^2\eta_\beta}\right) \tag{3}$$

where $J = M \times N$ is a parameter of the transmitter number and ϑ_I the standard deviation of the intensity in the rainfall. In Eq. (3), we have utilized the approximation in [21] for the mean of the irradiance fluctuations, i.e., the mean of the irradiance fluctuations is equal to one.

2.2. Model of Turbulent Fading Distribution

In weak scintillation regions and by the inverse Gaussian distribution [21], the distribution of the fading caused by turbulence of MIMO FSO systems can be described as

$$p\left(\eta_\alpha\right) = \sqrt{\frac{J^2}{2\pi\delta_I^2\eta_\alpha^3}}\exp\left(-\frac{\left(\eta_\alpha - J\right)^2}{2\delta_I^2\eta_\alpha}\right) \tag{4}$$

where δ_I is the standard deviation of the intensity [1] in Eq. (4), and the approximation of the mean of the irradiance fluctuations being one is utilized.

For non-Kolmogorov turbulence, the turbulent spectrum is given by [3, 24]

$$\phi_n\left(\alpha,\kappa\right) = A\left(\alpha\right)\tilde{C}_n^2\kappa^{-\alpha}, \quad 0 \le \kappa < \infty, \quad 3 < \alpha < 5 \tag{5}$$

where α is the spectral index of atmospheric turbulence, $A(\alpha) = \frac{1}{4\pi^2}\Gamma(\alpha-1)\cos(\alpha\pi/2)$, $\Gamma(x)$ the Gamma function, $\tilde{C}_n^2 = 0.033C_n^2(k/z)^{(\alpha-1/3)/2}/A(\alpha)$ the generalized refractive-index structure parameter of turbulent atmosphere with units $m^{-\alpha+11/3}$, C_n^2 the strength of the atmospheric turbulence, κ the scalar spatial wave number of turbulent fluctuations and $k = 2\pi/\lambda$ the optical wavenumber.

When a Gaussian-Schell electromagnetism beam propagates through the non-Kolmogorov turbulence channel over a distance z, the scintillation index [24, 25] is given by

$$\delta_I^2\left(\delta_{pe},z\right) \approx \frac{4.42\delta_{pe}^2\delta^2\left[\xi_s z_0/\left(r_0^2+\xi_s z_0^2\right)\right]^{\frac{\alpha}{2}-1}}{w_{LT}^2} + 3.86\delta^2\left(0.4\left[\left(1+2r_e\right)^2 + 4\left(\frac{\xi_s z_0}{r_0^2+\xi_s z_0^2}\right)^2\right]^{\frac{\alpha}{4}-\frac{1}{2}}\right.$$
$$\left.\times\cos\left[\frac{\alpha-2}{2}\tan^{-1}\left(\frac{\left(1+2r_e\right)\left(r_0^2+\xi_s z_0^2\right)}{2\xi_s z_0}\right)\right] - \frac{\alpha}{2\alpha-2}\left[\frac{\xi_s z_0}{r_0^2+\xi_s z_0^2}\right]^{\frac{\alpha}{2}-1}\right), \quad 3 < \alpha < 4 \tag{6}$$

where $z_0 = 2z/(kw_0^2)$, w_0 is the effective beam radius at the transmitter, and $r_0 = 1 - z/F_0$, F_0 is the phase curvature parameter of the beam at the transmitters; $r_e = r_0/(r_0^2 + \xi_s[\xi_s z_0/\xi_s {z_0}^2])$; $\xi_s = 1 + 2w_0^2/\rho_s^2$ is the source coherence parameter and ρ_s the spatial coherence length of the light source; $\delta^2 = -8\pi^2 A(\alpha)\alpha^{-1}\Gamma(1-\frac{\alpha}{2})\sin(\pi\alpha/4)\tilde{C}_n^2 k^{3-\alpha/2}z^{\alpha/2}$ is the Rytov variance of the plane wave in weak non-Kolmogorov turbulence [3, 26] and δ_{pe}^2 the variance of the beam wander caused by atmospheric turbulence.

The variance of the beam wander δ_{pe}^2 is given by

$$\delta_{pe}^2 = 219.6A\left(\alpha\right)\tilde{C}_n^2 z^3 w_0^{-1/3}\int_0^1 \frac{\xi^2}{\left[\left(1-z/F_0\right)+z\xi/F_0\right]^{4-\alpha}}$$
$$-\xi^2\left(\frac{\left(2\pi/r_{\alpha_0}\right)^2 w_0^2}{1+\frac{4\pi^2}{r_{\alpha_0}^2}w_0^2\left(\left(1-\frac{z}{F_0}\right)+\frac{z\xi}{F_0}\right)^2}\right)^{(2-\alpha/2)} d\xi \tag{7}$$

In Eq. (7), r_{α_0} represents the Fried's coherence diameter in non-Kolmogorov turbulence and is defined by [26]

$$r_{\alpha_0} = \left(\frac{2\left(\frac{8}{\alpha-2}\Gamma\left(\frac{2}{\alpha-2}\right)\right)^{\frac{\alpha-2}{2}}(\alpha-1)\,\Gamma\left(\frac{3-\alpha}{2}\right)}{\pi^{1/2}k^2\Gamma\left(\frac{2-\alpha}{2}\right)z\tilde{C}_n^2\left[\varepsilon+0.62\Lambda^{\alpha/2}\right]} \right)^{1/(\alpha-2)} \tag{8}$$

where $\Lambda = \frac{\Lambda_0}{\Theta_0^2+\Lambda_0^2}$, $\Theta_0 = 1-\frac{z}{F_0}$, $\Lambda_0 = \frac{2z}{kw_0^2}$, $\Theta = \frac{\Theta_0}{\Theta_0^2+\Lambda_0^2}$, $\varepsilon = \frac{1-\Theta^{\alpha-1}}{1-\Theta}$ $(\Theta \geq 0)$ or $\varepsilon = \frac{1+\Theta^{\alpha-1}}{1-\Theta}$ $(\Theta < 0)$, and $\rho_0^2(z,\alpha) = \left(\frac{-2^{3-\alpha}\pi^2\Gamma(1-\alpha/2)k^2A(\alpha)\tilde{C}_n^2z}{\Gamma(\alpha/2)}\right)^{-1/(\alpha-2)}$ is the spatial coherence radius of a spherical wave propagating in turbulent atmosphere [24].

2.3. Double IG Distribution of Raining Turbulence

The fading of raining turbulence can be modeled as

$$\eta_{\alpha\beta} = \eta_\alpha \eta_\beta \tag{9}$$

By the integral relationship [27] $\int_0^\infty x^{v-1}\exp(-\beta/x-\gamma x) = 2(\beta/\gamma)^v K_1(\sqrt{\beta\gamma}),\ (\beta>0,\gamma>0)$ [20], we have the double IG distribution of raining turbulence without pointing errors

$$\begin{aligned} p\left(\eta_{\alpha\beta}\right) &= \int_0^\infty p\left(\eta_{\alpha\beta}/\eta_\alpha\right)p\left(\eta_\alpha\right)d\eta_\alpha = \frac{J^2}{\pi\vartheta_I\delta_I}\exp\left(\frac{J\left(\delta_I^2+\vartheta_I^2\right)}{\vartheta_I^2\delta_I^2}\right)\sqrt{\frac{\eta_{\alpha\beta}\delta_I^2+\vartheta_I^2J^2}{\left(\eta_{\alpha\beta}\vartheta_I^2+\delta_I^2J^2\right)\eta_{\alpha\beta}^2}} \\ &\times K_1\left(\sqrt{\frac{\left(\eta_{\alpha\beta}\vartheta_I^2+\delta_I^2J^2\right)\left(\eta_{\alpha\beta}\delta_I^2+\vartheta_I^2J^2\right)}{\vartheta_I^4\delta_I^4\eta_{\alpha\beta}}}\right) \end{aligned} \tag{10}$$

where $K_v(z)$ is the modified Bessel function of the second kind.

2.4. Distribution of Raining Turbulence with Pointing Errors

In line-of-sight FSO communication links, pointing accuracy is an important issue in determining link performance and reliability [7]. Therefore, the effects of pointing errors caused by random building sways must be considered.

Consider a circular detection aperture of radius a and a Gaussian profile of the beam at the receiver. The attenuation due to geometric spread with pointing errors r is expressed as

$$\eta_p(r,z) \approx \left[erf\left(\frac{\sqrt{\pi}a}{\sqrt{2}w_{LT}}\right)\right]^2\exp\left(-\frac{2r^2}{w_{zeq}^2}\right) \tag{11}$$

where $w_{zep}^2 = \sqrt{\pi}w_{LT}^2(z)erf(\tilde{a}_{LT})(2\tilde{a}_{LT}\exp[-(\tilde{a}_{LT})^2])^{-1}$ is the equivalent beam width, $\tilde{a}_{LT} = \frac{\sqrt{2\pi}a}{2w_{LT}}$, $w_{LT}(z) = w_0[r_0^2+(\xi_s+\frac{2w_0^2}{\rho_0^2(z,\alpha)})(\frac{\lambda z}{\pi w_0^2})^2]^{1/2}$ the effective radius of the beam at receiving plane, and $erf(\bullet)$ the error function.

In the approximation of the independent identical Gaussian distributions for the elevation and the horizontal displacement [7], the probability distribution of pointing errors η_p can be expressed as

$$p\left(\eta_p\right) = \frac{\gamma^2}{A_0^{\gamma^2}}\eta_p^{\gamma^2-1}, \quad 0 \leq \eta_p \leq A_0 \tag{12}$$

where $A_0 = [erf(v)]^2$, $v = \frac{\sqrt{\pi}a}{\sqrt{2}w_{LT}}$, $\gamma = \frac{w_{zep}}{2\sigma_s}$ the ratio between the equivalent beam radius at the receiver and w_{zep} the standard deviation of the pointing errors at the receiver.

The probability distribution function $p(\eta_{\varpi n,\varpi_{LT}})$ of $\eta_{\varpi n} = \eta_{\alpha\beta}\eta_p$ can be written as [7]

$$p\left(\eta_{\varpi n},\varpi_{LT}\right) = \gamma^2A_0^{-\gamma^2}\eta_{\varpi n}^{\gamma^2-1}\int_{\eta/A_0}^\infty \eta_{\alpha\beta}^{-\gamma^2}p\left(\eta_{\alpha\beta}\right)d\eta_{\alpha\beta} \tag{13}$$

By the integral relationship

$$\int_0^\infty \exp\left(-\frac{a}{x}-\frac{x}{b}\right)dx = \sum_{m=0}^{\infty}\frac{(-1)^m}{b^m m!}a^{m+1}\Gamma\left(-m-1,0\right) \tag{14}$$

we have the distribution of raining turbulence with pointing errors

$$\begin{aligned} p\left(\eta_{\alpha\beta}\right) &= \frac{J^2}{\pi\vartheta_I\delta_I\eta_{\alpha\beta}^{3/2}}\exp\left(\frac{J\left(\delta_I^2+\vartheta_I^2\right)}{\vartheta_I^2\delta_I^2}\right)\sum_{m=0}^{\infty}\frac{(-1)^m\left(\eta_{\alpha\beta}\vartheta_I^2+\delta_I^2J^2\right)^m}{\left(2\eta_{\alpha\beta}\vartheta_I^2\delta_I^2\right)^m m!}\left(\frac{\eta_{\alpha\beta}\delta_I^2+\vartheta_I^2J^2}{2\vartheta_I^2\delta_I^2}\right)^{m+1} \\ &\quad\times\Gamma\left(-m-1,0\right) \end{aligned} \tag{15}$$

where $\Gamma(-m-1,0)$ is the incomplete gamma function.

By substituting Eq. (15) into Eq. (13), we obtain the double IG distribution of $\eta_{\alpha\beta}$ in raining turbulence with pointing errors

$$\begin{aligned} p\left(\eta_{\varpi n,\varpi_{LT}}\right) &= \frac{\gamma^2}{\pi}\exp\left(\frac{J\left(\delta_I^2+\vartheta_I^2\right)}{\vartheta_I^2\delta_I^2}\right)\sum_{m=0}^{\infty}(-1)^m\frac{1}{m!}\sum_{K=0}^{m}\binom{m}{K}\frac{J^{2K+2m+4}A_0^{1/2+K}\Gamma\left(-m-1,0\right)}{\vartheta_I^{2K+1}2^{2m+2}\delta_I^{4m-2K+3}\eta_{\varpi n}^{3/2+K}} \\ &\quad\times\frac{{}_2F_1\left(-\gamma^2-1/2-K,-m-1;-\gamma^2+1/2-K;-\dfrac{\delta_I^2\eta_{\varpi n}}{\vartheta_I^2J^2A_0}\right)}{\gamma^2+1/2+K} \end{aligned} \tag{16}$$

where ${}_pF_q\left(\bullet\right)$ is the hypergeometric series.

2.5. Outage Probability

By the definition of outage probability [3, 7], we obtain the outage probability of double IG raining turbulence channels.

$$\begin{aligned} p_{out}\left(\eta_0,w_{LT}\right) &= \int_0^{\eta_0}p\left(\eta_{\varpi n},w_{LT}\right)d\eta_{\varpi n} = \frac{\gamma^2}{\pi}\exp\left(\frac{J\left(\delta_I^2+\vartheta_I^2\right)}{\vartheta_I^2\delta_I^2}\right)\sum_{m=0}^{\infty}(-1)^m\frac{1}{m!}\sum_{K=0}^{m}\binom{m}{K} \\ &\quad\times\frac{J^{2K+2m+4}A_0^{1/2+K}\left(\dfrac{1}{2}\right)^{2m+2}\Gamma\left(-m-1,0\right)}{\left(\gamma^2+1/2+K\right)\vartheta_I^{2K+1}\delta_I^{4m-2K+3}\eta_0^{1/2+K}}\Gamma\left(-1/2-K\right) \\ &\quad\times{}_3F_2\left(-\frac{1}{2}-K,-\gamma^2-\frac{1}{2}-K;\frac{1}{2}+K,-\gamma^2+\frac{1}{2}-K,-\frac{\delta_I^2\eta_0}{\vartheta_I^2J^2A_0}\right) \end{aligned} \tag{17}$$

where η_0 is the threshold value of the instantaneous intensity gain.

2.6. Average BER

Using the optimum decision metric for OOK and the assuming of perfect channel state information, the average BER of the MIMO FSO communication system is given by [1, 16].

$$P_{BER} = \frac{1}{2}\int_0^\infty p\left(\eta_{\varpi n},w_{LT}\right)erfc\left(\frac{\tau\eta_{\varpi n}}{2\sqrt{2}MN\sigma_h}\right)d\eta_{\varpi n} \tag{18}$$

By substituting Eq. (16) into Eq. (18) and using the Merjer's functions expression of $erfc(\bullet)$, i.e., $erfc(\sqrt{x}) = \frac{1}{\sqrt{\pi}}G_{1,2}^{2,0}\left(x|_{0,1/2}^{1}\right)$ we can express Eq. (18) as

$$\begin{aligned} P_{BER} &= \frac{\gamma^2}{\pi^{5/2}}\exp\left(\frac{J\left(\delta_I^2+\vartheta_I^2\right)}{\vartheta_I^2\delta_I^2}\right)\sum_{m=0}^{\infty}(-1)^m\frac{1}{m!}\sum_{K=0}^{m}\binom{m}{K} \\ &\quad\times\frac{J^{2m+3}\Gamma\left(-m-1,0\right)\left(\gamma^2+1/2+K\right)^{-1}}{2^{m-1}\delta_I^{4m-4K+2}\vartheta_I^{4K+2}\Gamma\left(-\gamma^2-1/2-K\right)\Gamma\left(-m-1\right)} \end{aligned}$$

$$\times G_{5,6}^{6,2}\left(\frac{\vartheta_I^4\tau^2J^2A_0^2}{8\sigma_h^2\delta_I^2}\;\middle|\;\begin{matrix}1,\dfrac{3/2+K}{2},\dfrac{5/2+K}{2},\dfrac{2+\gamma^2}{2},\dfrac{3+\gamma^2}{2}\\ 0,\dfrac{1}{2},\dfrac{\gamma^2}{2},\dfrac{1+\gamma^2}{2},\dfrac{K-1/2-m}{2},\dfrac{K+1/2-m}{2}\end{matrix}\right) \tag{19}$$

3. NUMERICAL RESULTS AND DISCUSSION

In this section, we present the numerical discussions for the outage probability and average BER as a function of the coherent length of the source, pointing error, radius of detection aperture, effective emitting radius, number of transmitters and receivers, spectral index and scintillation index of rainfall and turbulence. The system parameters are settled as the wavelength $\lambda = 1550\,\text{nm}$, curvature radius of beam phase front at transmitter $F_0 = \infty$ (the collimated beam), noise standard deviation $\sigma_h = 1 \times 10^{-7}\,\text{A/Hz}$, detection efficiency $\tau = 1$, and threshold value of instantaneous intensity gain $\eta_0 = 0.5$.

Figure 2(a) shows outage probability curves, and Figure 2(b) shows BER curves as a function of the scintillation index of rainfall and turbulence. The outage probability and BER increase with the increase of the scintillation index of rainfall and turbulence. In the small scintillation index of turbulence, the outage probability and BER increase tardily with increasing the scintillation index of turbulence. However, for larger scintillation index of turbulence, the outage probability and BER change quickly. In addition, the increase of BER with increasing the scintillation index of rainfall is analogous to the increase of BER with increasing the scintillation index of turbulence, but the outage probability nearly linearly increases with increasing the scintillation index of rainfall. We find that the effects of turbulence on BER are greater than that of rainfall for $\delta_I^2 = \vartheta_I^2$. Nevertheless, the effects of rainfall on outage probability are greater than that of turbulence for $\delta_I^2 = \vartheta_I^2$.

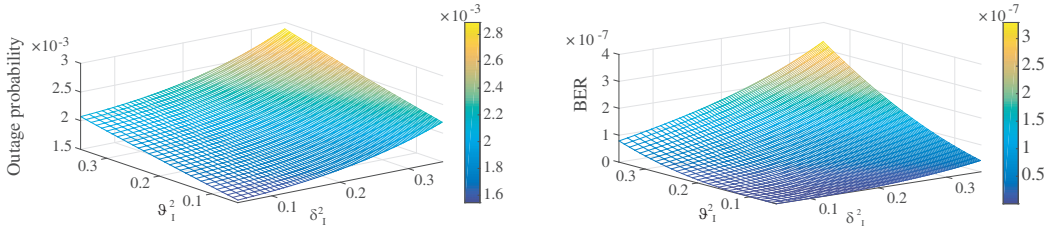

Figure 2. Outage probability (Figure 2(a)) and BER (Figure 2(b)) of MIMO communication systems for the different scintillation index of rainfall or turbulence with the radius of detection aperture $a = 0.18\,\text{m}$, the coherent length of source $\rho_s = 0.02\,\text{m}$, the transmitter number $M = 2$, the propagation distance $z = 2000\,\text{m}$, the receiver number $N = 2$, the spectral index $\alpha = 3.67$, the effective beam radius at the transmitter $w_0 = 0.1\,\text{m}$, the refractive-index construction parameter $C_n^2 = 1 \times 10^{-15}\,\text{m}^{-2/3}$, the pointing error standard variance $\sigma_s = 0.3$.

Figure 3(a) and Figure 3(b) plot the outage probability and BER under different spatial coherence lengths of the source and radii of detection aperture. When the coherence length of light sources is less than the transmitting aperture radius (0.1 m), BER and outage probability primitively increase with the increase of the coherence length of light sources. As the coherence length of light sources exceeds the transmitting aperture radius (0.1 m), BER and outage probability increase to saturation. Our results show that the spatially partially coherent beam has considerable improvement on the outage probability and BER. The outage probability and BER associated with the radius of detection aperture are shown in Figure 3. When the radius of the detection is less than 0.12 m, the outage probability and BER fluctuate with the increase of radius of the detection. As the radius of the detection increases more than 0.12 m, the outage probability and BER reduce rapidly due to aperture averaging effects working. The case of a large-aperture receiver shows considerable improvement in the predicted the outage probability and BER.

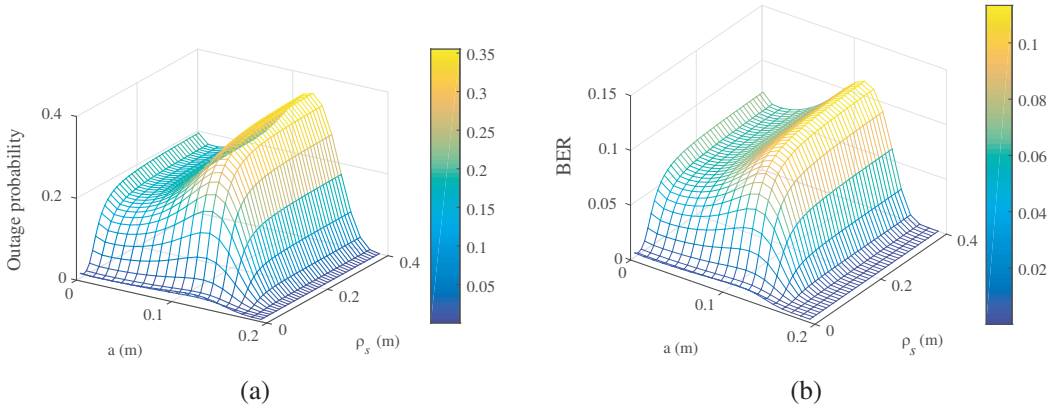

(a) (b)

Figure 3. Outage probability (Figure 3(a)) and BER (Figure 3(b)) of MIMO communication systems versus different values of the spatial coherence length of the source ρ_s and the detection aperture of radius a with the transmitter number $M = 2$, the receiver number $N = 2$, the spectral index $\alpha = 3.67$, the scintillation index of rainfall $\vartheta_I^2 = 0.1$, the propagation distance $z = 1000\,\mathrm{m}$, the effective beam radius at the transmitter $w_0 = 0.1\,\mathrm{m}$, the refractive-index construction parameter $C_n^2 = 1 \times 10^{-15}\,\mathrm{m}^{-2/3}$, and the pointing errors standard variance $\sigma_s = 0.15$.

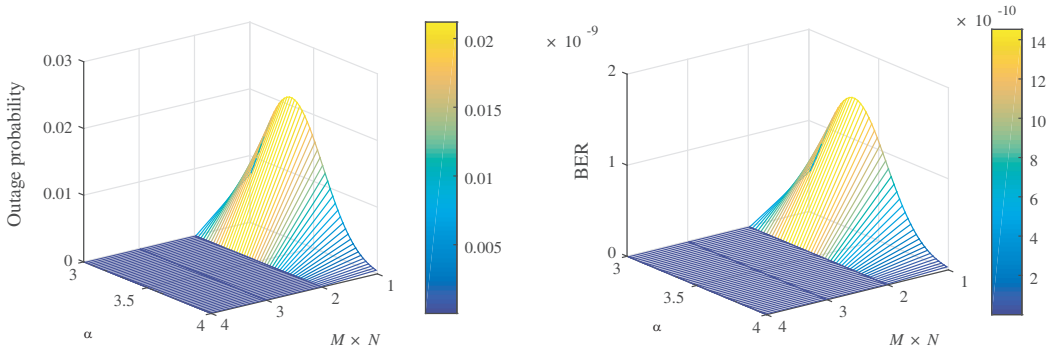

(a) (b)

Figure 4. Outage probability (Figure 4(a)) and BER (Figure 4(b)) of MIMO communication systems versus different values of the transmitter number M, the receiver number N, and the spectral index α with the coherent length of source $\rho_s = 0.01\,\mathrm{m}$, the radius of detection aperture $a = 0.02\,\mathrm{m}$, the scintillation index of rainfall $\vartheta_I^2 = 0.1$, the propagation distance $z = 1000\,\mathrm{m}$, the effective beam radius at the transmitter $w_0 = 0.04\,\mathrm{m}$, the pointing errors standard variance $\sigma_s = 0.15$, and the refractive-index construction parameter $C_n^2 = 1 \times 10^{-15}\,\mathrm{m}^{-2/3}$.

In Figure 4, the outage probability and BER versus M, N and the spectral index α are depicted. Figure 4(a) and Figure 4(b) show that the outage probability and BER increase to maximum with increasing index of α non-Kolmogorov turbulence from 3.0 to 3.3, and they decrease with increasing α from 3.3 to 4.0. The result can be derived from the fluctuation pattern of beam wavefront with the increase of α [28]. In addition, Figure 4(a) and Figure 4(b) show the increase of the receiver or transmitter number is helpful to reducing the outage probability and BER of the system. Moreover, we see that the outage probability and BER can be reduced by several orders of magnitude by increasing the number of apertures from one to four, given a fixed value of the spectral index. A similar observation is made concerning a coherent array of receivers established by experimental data [29].

Given the radius of receiving aperture, the effects of pointing errors and effective emitting apertures on the outage probability and BER are shown in Figure 5. The outage probability and BER increase to maximum with increasing pointing errors, and decrease tardily with the sequential increase of pointing errors. Meanwhile, the outage probability and BER increase initially with the increase of the effective

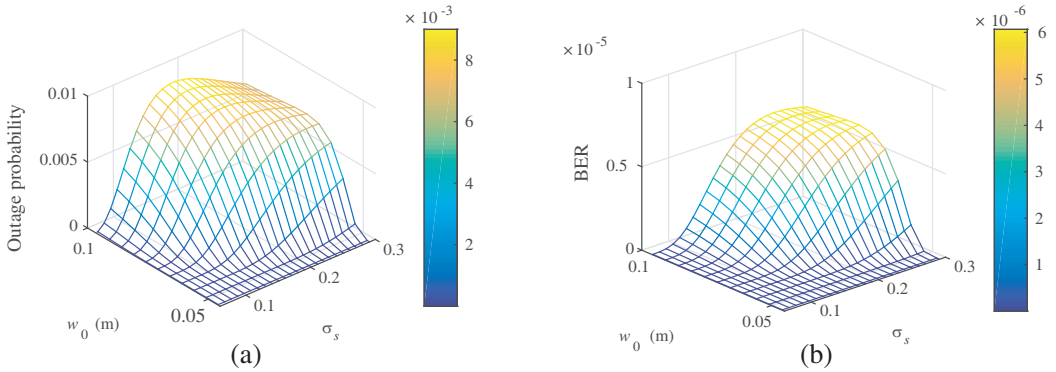

Figure 5. Outage probability (Figure 5(a)) and BER (Figure 5(b)) of MIMO communication systems versus the effective beam radius w_0 and the pointing errors standard deviation σ_s, the scintillation index of rainfall $\vartheta_I^2 = 0.1$, the radius of detection aperture $a = 0.1\,\mathrm{m}$, the transmitter numbers M, the receiver numbers N, the coherent length of source $\rho_s = 0.02\,\mathrm{m}$, the propagation distance $z = 1000\,\mathrm{m}$, the refractive-index construction parameter $C_n^2 = 1 \times 10^{-15}\,\mathrm{m}^{-2/3}$, and the spectral index $\alpha = 3.67$.

emitting radius, then increase tardily with the sequential increase of the effective emitting radius. The phenomena result from the increase of the beam diameter can reduce beam jitter and beam spread caused by raining turbulence. These results also show that the increase of effective emitting apertures can reduce effects of pointing errors and beam jitter on the outage probability and BER of the raining turbulence link.

4. CONCLUSION

In this work, we have established the double IG probability distribution function of the raining turbulence fading, outage probability and average BER for MIMO FSO links with Gaussian-Schell electromagnetism beams in weak scintillation atmosphere with rainfall. We find that the effects of turbulence on BER is greater than that of rainfall for $\delta_I^2 = \vartheta_I^2$, but the effects of rainfall on outage probability are greater than that of turbulence for $\delta_I^2 = \vartheta_I^2$. The increase of the receiver or transmitter number is helpful to reducing the outage probability and BER of the system. The increase of the effective emitting aperture reduces the effects of pointing errors and beam jitter on the outage probability and BER of the raining turbulence link. Further work needs to be carried out to establish the average BER of MIMO FSO links in raining turbulence without the assumption of perfect channel state information.

ACKNOWLEDGMENT

This work is supported by the the Natural Science Foundation of Jiangsu Province of China (Grant No. BK20140128), the Fundamental Research Funds for the Central Universities (JUSRP51517) and the graduate student research innovation project of Jiangsu province general university (Grant No. KYLX_151187).

REFERENCES

1. Majumdar, A. K., *Advanced Free Space Optics (FSO): A System Approach*, Springer, New York, 2014.
2. Andrews, L. and R. L. Phillips, *Laser Beam Propagation Through Random Media*, SPIE, Bellingham, WA, 2005.
3. Zhang, Y. X., C. Si, Y. Wang, J. Wang, and J. Jia, "Capacity for non-Kolmogorov turbulent optical links with beam wander and pointing errors," *J. Opt. Laser Techno.*, Vol. 43, No. 7, 1338–1342, 2011.

4. Yu, J. Y., Y. H. Chen, L. Liu, X. L. Liu, and Y. J. Cai, "Splitting and combining properties of an elegant Hermite-Gaussian correlated Schell-model beam in Kolmogorov and non-Kolmogorov turbulence," *Opt. Express*, Vol. 23, No. 10, 13467–13481, 2015.
5. Baykal, Y. and H. Gerçekcioğlu, "Application of equivalent structure constant in scintillations and BER found for non-Kolmogorov spectrum," *Opt. Commun.*, Vol. 310, 109–113, 2014.
6. Eyyuboğlu, H. T., "Apertured averaged scintillation of fully and partially coherent Gaussian, annular Gaussian, flat toped and dark hollow beams," *Opt. Commun.*, Vol. 339, 141–147, 2015.
7. Farid, A. A. and S. Hranilovic, "Outage capacity optimization for free-space optical links with pointing errors," *J. Lightw. Technol.*, Vol. 25, No. 7, 1702–1710, 2007.
8. Grabner, M. and V. Kvicera, "Multiple scattering in rain and fog on free-space optical links," *J. Lightw. Technol.*, Vol. 32, No. 3, 513–520, 2014.
9. Lin, S. H., "A method for calculating rain attenuation distributions on microwave paths," *Bell Syst. Tech. J.*, Vol. 54, No. 6, 1051–1083, 1975.
10. Morita, K. and I. Higuti, "Prediction methods for rain attenuation distributions of micro and millimeter waves," *Rev. Electron. Commun. Labs*, Vol. 24, No. 7, 651–668, 1976.
11. Livieratos, S., V. Katsambas, and J. D. Kanellopoulos, "A Global method for the prediction of the slant path rain attenuation statistics," *Journal of Electromagnetic Waves and Applications*, Vol. 14, No. 5, 713–724, 2000.
12. Panagopoulos, A. D., P. D. M. Arapoglou, J. D. Kanellopoulos, and P. G. Cottis, "Long-term rain attenuation probability and site diversity gain prediction formulas," *IEEE Trans. Antennas Propag.*, Vol. 53, No. 7, 2307–2313, 2005.
13. Kourogiorgas, C., A. D. Panagopoulos, and J. D. Kanellopoulos, "On the earth-space site diversity modeling: A novel physical-mathematical outage prediction model," *IEEE Trans. Antennas Propag.*, Vol. 60, No. 9, 4391–4397, 2012.
14. Kourogiorgas, C., "A new method for the prediction of outage probability of LOS terrestrial links operating above 10 GHz," *IEEE Antenn. Wireless Propaga. Lett.*, Vol. 12, 516–519, 2013.
15. Kourogiorgas, C. and A. D. Panagopoulos, "New physical-mathematical model for predicting slant-path rain attenuation statistics based on inverse Gaussian distribution," *IET Microw. Antennas Propag.*, Vol. 7, No. 12, 970–975, 2013.
16. Navidpour, S. M., M. Uysal, and M. Kavehrad, "BER performance of free-space optical transmission with spatial diversity," *IEEE Tran. Wireless Commun.*, Vol. 6, No. 8, 2813–2819, 2007.
17. Chatzidiamantis, N. D. and H. G. Sanddalidis, "Inverse Gaussian modeling of turbulence-induced fading in free-space optical systems," *J. Lightw. Technol.*, Vol. 29, No. 10, 1590–1596, 2011.
18. Wang, F., Y. Cai, H. T. Eyyuboğlu, and Y. Baykal, "Average intensity and spreading of partially coherent standard and elegant laguerre-gaussian beams in turbulent atmosphere," *Progress In Electromagnetics Research*, Vol. 103, 33–56, 2010.
19. Li, Y. Q., Z.-S. Wu, and L. G. Wang, "Polarization characteristics of a partially coherent gaussian schell-model beam in slant atmospheric turbulence," *Progress In Electromagnetics Research*, Vol. 121, 453–468, 2011.
20. Wang, F., X. Liu, and Y. Cai, "Propagation of partially coherent beam in turbulent atmosphere: A review," *IEEE Trans. Commun.*, Vol. 150, 123–143, 2015.
21. Trigui, I., A. Laourine, S. Affes, and A. Stephenne, "The inverse Gaussian distribution in wireless channels: Second-order statistics and channel capacity," *IEEE Trans. Commun.*, Vol. 60, No. 11, 3167–3173, 2012.
22. Karmeshu and R. Agrawal, "On efficacy of Rayleigh-inverse Gaussian distribution over K-distribution for wireless fading channels," *Wireless Commun. Mobile Comput.*, Vol. 7, No. 1, 1–7, 2007.
23. Mohammed, N. A., A. S. El-Wakeel, and M. H. Aly, "Performance evaluation of FSO link under NRZ-RZ line codes, different weather conditions and receiver types in the presence of pointing errors," *J. Elec. Electronic Enginee.*, Vol. 6, No. 12, 28–35, 2012.

24. Deng, P., M. Kavehrad, Z. Liu, Z. Zhou, and X. Yuan, "Capacity of MIMO free space optical communications using multiple partially coherent beams propagation through non-Kolmogorov strong turbulence," *Opt. Express*, Vol. 21, No. 13, 15213–15229, 2013.
25. Borah, D. K. and D. G. Voelz, "Spatially partially coherent beam parameter optimization for free space optical communications," *Opt. Express*, Vol. 18, No. 20, 20746–20758, 2010.
26. Toselli, I., L. C. Andrews, R. L. Phillips, and V. Ferrero, "Free-space optical system performance for laser beam propagation through non-Kolmogorov turbulence," *Opt. Enginee.*, Vol. 47, No. 2, 026003, 2008.
27. Wolfram, Wolfram function site, 2010, Available: http://function.wolfram.com.
28. Huang, Y., A. Zeng, Z. Gao, and B. Zhang, "Beam wander of partially coherent array beams through non-Kolmogorov turbulence," *Opt. Lett.*, Vol. 40, No. 8, 1619–1622, 2015.
29. Andrews, L. C., R. L. Phillips, and C. Y. Hopen, *Laser Beam Scintillation With Applications*, SPIE, Bellingham, WA, 2001.